

# Triplet vector boson and the flavor anomalies: flavor and collider constraints

Presented by Eduardo Rojas

In collaboration with: José Miguel Cabarcas, José Herman Muñoz,  
Nestor Quintero Poveda

VII UNIANDES PARTICLE PHYSICS SCHOOL, Bogotá 2022

Universidad de Nariño



eduro4000@gmail.com

December 13, 2022

# Outline

- 1 The Triplet Vector boson model
- 2 Effective Lagrangian
- 3 Relevant Observables
- 4 Projections
- 5 Results
- 6 Conclusions

# The Triplet Vector boson model

In general, flavor anomalies have been boarded into the current literature as a motivation to build innovative models and to test well established New Physics (NP) models. In this section, we focus in the previously mentioned Triplet Vector Boson (TVB) model [1, 2, 3, 4, 5, 6, 7, 8] as a possible explanations of these anomalies, that might accommodate the observed flavor experimental results.

In the fermion mass basis, the most general lagrangian describing the dynamics of the fields can be written as

$$\Delta\mathcal{L}_V = g_{ij}^q(\bar{\Psi}_{iL}^Q\gamma^\mu\sigma^I\Psi_{jL}^Q)V_\mu^I + g_{ij}^\ell(\bar{\Psi}_{iL}^\ell\gamma^\mu\sigma^I\Psi_{jL}^\ell)V_\mu^I \quad (1)$$

where,  $V_\mu$  stands for the extra or new vector bosons that transform as (1, 3, 0) under the  $SU(3)_C \otimes SU(2)_L \otimes U(1)_Y$  gauge symmetry and must be redefined as  $W'^{\pm}, Z'$ .

# The Triplet Vector boson model

On other side, SM fermions are arranged into the doublets  $\Psi_L^Q$  and  $\Psi_L^\ell$  given by

$$\Psi_L^Q = \begin{pmatrix} V^\dagger u_L \\ d_L \end{pmatrix}, \quad \Psi_L^\ell = \begin{pmatrix} \nu_L \\ \ell_L \end{pmatrix}. \quad (2)$$

It is worth noticing here that in this particular model the CKM mixing matrix  $V$  is applied on the up-type quarks.

# Effective Lagrangian

$$\begin{aligned}
 \frac{g_{ij}^q g_{kl}^\ell J_Q J_\ell}{M_V^2} &= 2 \frac{g_{kl}^\ell}{M_V^2} \left[ (Vg^d)_{ij} (\bar{u}_{iL} \gamma_\mu d_{jL}) (\bar{\ell}_k \gamma^\mu \nu_{lL}) + \text{h.c.} \right] \\
 &+ \frac{g_{kl}^\ell}{M_V^2} \left[ (Vg^d V^\dagger)_{ij} (\bar{u}_{iL} \gamma_\mu u_{jL}) (\bar{\nu}_{kL} \gamma^\mu \nu_{lL}) + g_{ij}^d (\bar{d}_{iL} \gamma_\mu d_{jL}) (\bar{\ell}_{kL} \gamma^\mu \ell_{lL}) \right] \\
 &- \frac{g_{kl}^\ell}{M_V^2} \left[ (Vg^d V^\dagger)_{ij} (\bar{u}_{iL} \gamma_\mu u_{jL}) (\bar{\ell}_{kL} \gamma^\mu \ell_{lL}) + g_{ij}^d (\bar{d}_{iL} \gamma_\mu d_{jL}) (\bar{\nu}_{kL} \gamma^\mu \nu_{lL}) \right],
 \end{aligned}$$

in this expression, we can identify that the first term expresses an effective interaction of the SM fields that should be mediated by extra bosonic charged fields, while the remaining terms are mediated by an extra neutral bosonic field.

# $b \rightarrow c \ell^- \bar{\nu}_\ell$ ( $\ell = \mu, \tau$ ) data

The  $W'$  boson leads to additional tree-level contribution to  $b \rightarrow c \ell^- \bar{\nu}_\ell$  transitions involving leptons from second- and third-generation ( $\ell = \mu, \tau$ ). The total low-energy effective Lagrangian has the following form [9]

$$-\mathcal{L}_{\text{eff}}(b \rightarrow c \ell \bar{\nu}_\ell)_{\text{SM}+W'} = \frac{4G_F}{\sqrt{2}} V_{cb} \left[ (1 + C_V^{bc\ell\nu_\ell})(\bar{c}\gamma_\mu P_L b)(\bar{\ell}\gamma^\mu P_L \nu_\ell) \right],$$

where  $G_F$  is the Fermi coupling constant,  $V_{cb}$  is the charm-bottom Cabbibo-Kobayashi-Maskawa (CKM) matrix element, and  $C_V^{bc\ell\nu_\ell}$  is the Wilson coefficient (WC) associated with the NP vector (left-left) operator. This WC is defined as

$$C_V^{bc\ell\nu_\ell} = \frac{\sqrt{2}}{4G_F V_{cb}} \frac{2(V_{cs}g_{sb}^q + V_{cb}g_{bb}^q)g_{\ell\ell}^\ell}{M_V^2} \quad (\ell = \mu, \tau),$$

with  $M_V$  the heavy boson mass.

# $b \rightarrow c \ell^- \bar{\nu}_\ell$ ( $\ell = \mu, \tau$ ) data

The NP effects on the LFU ratios  $R(X)$  ( $X = D, D^*, J/\psi$ ), the  $D^*$  and  $\tau$  longitudinal polarizations related with the channel  $\bar{B} \rightarrow D^* \tau \bar{\nu}_\tau$ , the ratio of inclusive decays  $R(X_c) \equiv \text{BR}(B \rightarrow X_c \tau \bar{\nu}_\tau) / \text{BR}(B \rightarrow X_c \mu \bar{\nu}_\mu)$ , and the tauonic decay  $B_c^- \rightarrow \tau^- \bar{\nu}_\tau$  can be easily parametrized as [9, 10]

$$R(X) = R(X)_{\text{SM}} |1 + C_V^{bc\tau\nu\tau}|^2, \quad (3)$$

$$F_L(D^*) = F_L(D^*)_{\text{SM}} r_{D^*}^{-1} |1 + C_V^{bc\tau\nu\tau}|^2, \quad (4)$$

$$P_\tau(D^*) = P_\tau(D^*)_{\text{SM}} r_{D^*}^{-1} |1 + C_V^{bc\tau\nu\tau}|^2, \quad (5)$$

$$R(X_c) = R(X_c)_{\text{SM}} \left( 1 + 2.294 \text{Re}(C_V^{bc\tau\nu\tau}) + 1.147 |C_V^{bc\tau\nu\tau}|^2 \right), \quad (6)$$

$$\text{BR}(B_c^- \rightarrow \tau^- \bar{\nu}_\tau) = \text{BR}(B_c^- \rightarrow \tau^- \bar{\nu}_\tau)_{\text{SM}} |1 + C_V^{bc\tau\nu\tau}|^2, \quad (7)$$

respectively, where  $r_{D^*} = R(D^*) / R(D^*)_{\text{SM}}$ . For  $\text{BR}(B_c^- \rightarrow \tau^- \bar{\nu}_\tau)$ , we will use the bound  $< 10\%$  [11].

# Semileptonic decay $\Lambda_c \rightarrow \Lambda_c \tau \nu_\tau$

Concerning to the ratio  $R(\Lambda_c)$  very recently measured by LHCb (LHCb:2022piu), the SM contribution is also rescaled by the overall factor  $|1 + C_V^{bc\tau\nu_\tau}|^2$ , namely (Datta:2017aue)

$$R(\Lambda_c) = R(\Lambda_c)_{\text{SM}} |1 + C_V^{bc\tau\nu_\tau}|^2. \quad (8)$$



# $b \rightarrow s\mu^+\mu^-$ data

The NP effective Lagrangian responsible for the semileptonic transition  $b \rightarrow s\mu^+\mu^-$  can be expressed as

$$\mathcal{L}(b \rightarrow s\mu^+\mu^-)_{\text{NP}} = \frac{4G_F}{\sqrt{2}} V_{tb} V_{ts}^* (C_9^{bs\mu\mu} \mathcal{O}_9^{bs\mu\mu} + C_{10}^{bs\mu\mu} \mathcal{O}_{10}^{bs\mu\mu}) + \text{h.c.},$$

where the NP is encoded in the WCs  $C_9^{bs\mu\mu}$  and  $C_{10}^{bs\mu\mu}$  of the four-fermion operators

$$\mathcal{O}_9^{bs\mu\mu} = \frac{\alpha_{\text{em}}}{4\pi} (\bar{s}\gamma_\mu P_L b)(\bar{\mu}\gamma^\mu \mu),$$

$$\mathcal{O}_{10}^{bs\mu\mu} = \frac{\alpha_{\text{em}}}{4\pi} (\bar{s}\gamma_\mu P_L b)(\bar{\mu}\gamma^\mu \gamma_5 \mu),$$

respectively. Several global analyses of the most current  $b \rightarrow s\mu^+\mu^-$  data have been recently performed suggesting various NP interpretations [12, 13, 14, 15, 16, 17, 18, 19].

# Wilson coefficients

respectively. Several global analyses of the most current  $b \rightarrow s\mu^+\mu^-$  data have been recently performed suggesting various NP interpretations [12, 13, 14, 15, 16, 17, 18, 19]. Among the NP scenarios, the  $C_9^{bs\mu\mu} = -C_{10}^{bs\mu\mu}$  solution is strongly preferred by the data. In our analysis we will take into account the results obtained by Altmannshofer and Stangl [13], in which the best fit  $1\sigma$  solution leads to

$$C_9^{bs\mu\mu} = -C_{10}^{bs\mu\mu} \in [-0.46, -0.32]. \quad (9)$$

In the context of the TVB model, the  $Z'$  boson induces a tree-level contribution to  $b \rightarrow s\mu^+\mu^-$  transition via the WCs

$$C_9^{bs\mu\mu} = -C_{10}^{bs\mu\mu} = -\frac{\pi}{\sqrt{2}G_F\alpha_{\text{em}}V_{tb}V_{ts}^*} \frac{g_{sb}^q g_{\mu\mu}^\ell}{M_V^2}. \quad (10)$$

Using the result of the global fit, Eq. (9), this corresponds to

$$-\frac{g_{sb}^q g_{\mu\mu}^\ell}{M_V^2} \in [4.8, 6.9] \times 10^{-4} \text{ TeV}^{-2}. \quad (11)$$

# Bottomonium processes: $R_{\Upsilon(nS)}$ and $\Upsilon \rightarrow \mu^\pm \tau^\mp$

Test of LFU has been also studied in the leptonic ratio  $R_{\Upsilon(nS)}$  (with  $n = 1, 2, 3$ ) in connection with the reported hints of LFU violation in the charged-current transition  $b \rightarrow c \tau \bar{\nu}_\tau$  [20, 10]. It is known that NP scenarios aiming to provide an explanation to the anomalous  $b \rightarrow c \tau \bar{\nu}_\tau$  data, also induce effects in the neutral-current transition  $b\bar{b} \rightarrow \tau^+ \tau^-$  [20, 10]. Experimentally, the BABAR and CLEO Collaborations have reported the values [21, 22, 23]

$$R_{\Upsilon(1S)} = \begin{cases} \text{BABAR-10: } 1.005 \pm 0.013 \pm 0.022 \text{ [21]}, \\ \text{SM: } 0.9924 \text{ [20]}, \end{cases}$$

$$R_{\Upsilon(2S)} = \begin{cases} \text{CLEO-07: } 1.04 \pm 0.04 \pm 0.05 \text{ [22]}, \\ \text{SM: } 0.9940 \text{ [20]}, \end{cases}$$

$$R_{\Upsilon(3S)} = \begin{cases} \text{CLEO-07: } 1.05 \pm 0.08 \pm 0.05 \text{ [22]}, \\ \text{BABAR-20: } 0.966 \pm 0.008 \pm 0.014 \text{ [23]}, \\ \text{SM: } 0.9948 \text{ [20]}, \end{cases}$$

# Bottomonium processes: $R_{\Upsilon(nS)}$ and $\Upsilon \rightarrow \mu^\pm \tau^\mp$

where the theoretical uncertainty is typically of the order  $\pm \mathcal{O}(10^{-5})$  [20]. These measurements are in good accordance with the SM estimations, except for the 2020 measurement on  $R_{\Upsilon(3S)}$  that shows an agreement at the  $1.8\sigma$  level [23]. By averaging the CLEO-07 [22] and BABAR-20 [23] measurements we obtain  $R_{\Upsilon(3S)}^{\text{Ave}} = 0.968 \pm 0.016$ , which deviates at the  $1.7\sigma$  level with respect to the SM prediction [10].

The NP effects of the TVB model on the leptonic ratio can be expressed as [20, 10]

$$R_{\Upsilon(nS)} = \frac{(1 - 4x_\tau^2)^{1/2}}{|A_V^{\text{SM}}|^2} \left[ |A_V^{b\tau}|^2 (1 + 2x_\tau^2) + |B_V^{b\tau}|^2 (1 - 4x_\tau^2) \right],$$

with  $x_\tau = m_\tau/m_{\Upsilon(nS)}$ ,  $|A_V^{\text{SM}}| = -4\pi\alpha Q_b$ , and

$$\begin{aligned} A_V^{b\tau} &= -4\pi\alpha Q_b + \frac{m_{\Upsilon(nS)}^2}{4} \frac{g_{bb}^q g_{\tau\tau}^\ell}{4M_V^2}, \\ B_V^{b\tau} &= -\frac{m_{\Upsilon(nS)}^2}{2} \frac{g_{bb}^q g_{\tau\tau}^\ell}{4M_V^2}. \end{aligned}$$

# $\Delta F = 2$ processes: $B_s - \bar{B}_s$ and $D^0 - \bar{D}^0$ mixing

The interactions of a  $Z'$  boson to quarks  $s\bar{b}$  relevant for  $b \rightarrow s\mu^+\mu^-$  processes also generate a contribution to  $B_s - \bar{B}_s$  mixing [24, 25]. The NP effects to the  $B_s - \bar{B}_s$  mixing can be described by the effective Lagrangian

$$\mathcal{L}_{\Delta B=2}^{Z'} = -\frac{4G_F}{\sqrt{2}} |V_{tb}V_{ts}^*|^2 C_{sb}^{LL} (\bar{s}\gamma_\mu P_L b)(\bar{s}\gamma^\mu P_L b) + \text{h.c.}, \quad (12)$$

where

$$C_{sb}^{LL} = \frac{1}{4\sqrt{2}G_F |V_{tb}V_{ts}^*|^2} \frac{|g_{sb}^q|^2}{M_{Z'}^2}. \quad (13)$$

Thus, the NP contributions to the mass difference  $\Delta M_s$  of the neutral  $B_s$  meson can be expressed as [24]

$$\frac{\Delta M_s^{\text{SM+NP}}}{\Delta M_s^{\text{SM}}} = \left(1 + \frac{\eta^{6/23}}{R_{\text{SM}}^{\text{loop}}} C_{sb}^{LL}\right), \quad (14)$$

where  $\eta = \alpha_s(M_{Z'})/\alpha_s(m_b)$  accounts for running from the  $M_{Z'}$  scale down to the  $b$ -quark mass scale and the SM loop function is  $R_{\text{SM}}^{\text{loop}} = (1.310 \pm 0.010) \times 10^{-3}$  [24]. At present,  $\Delta M_s$  has been experimentally measured with great precision  $\Delta M_s^{\text{Exp}} = (17.757 \pm 0.021) \text{ ps}^{-1}$  [24, 26].

$\Delta F = 2$  processes:  $B_s - \bar{B}_s$  and  $D^0 - \bar{D}^0$  mixing

On the theoretical side, the most recent 2019 average is  $\Delta M_s^{\text{SM}} = (18.4_{-1.2}^{+0.7}) \text{ ps}^{-1}$  implying that  $\Delta M_s^{\text{SM}} / \Delta M_s^{\text{Exp}} = 1.04_{-0.07}^{+0.04}$  [24]. This value yields to

$$0.89 \leq \left| 1 + \frac{\eta^{6/23}}{R_{\text{loop}}^{\text{SM}}} C_{sb}^{LL} \right| \leq 1.11, \quad (15)$$

where in the TVB model translates into the important  $2\sigma$  bound

$$\frac{|g_{sb}^q|}{M_V} \geq 3.9 \times 10^{-3} \text{ TeV}^{-1}. \quad (16)$$

# Analysis on the TVB parametric space

In this section we present the parametric space analysis of the TVB model addressing a simultaneous explanation of the  $b \rightarrow s\mu^+\mu^-$  and  $b \rightarrow c\tau\bar{\nu}_\tau$  anomalies. We define the pull for the  $i$ -th observable as

$$\text{pull}_i = \frac{\mathcal{O}_i^{\text{exp}} - \mathcal{O}_i^{\text{th}}}{\Delta\mathcal{O}_i}, \quad (17)$$

where  $\mathcal{O}_i^{\text{exp}}$  is the experimental measurement,  $\mathcal{O}_i^{\text{th}} \equiv \mathcal{O}_i^{\text{th}}(g_{bs}^q, g_{bb}^q, g_{\mu\mu}^\ell, g_{\tau\tau}^\ell, g_{\mu\tau}^\ell)$  is the theoretical prediction that include the NP contributions, and  $\Delta\mathcal{O}_i = ((\sigma_i^{\text{exp}})^2 + (\sigma_i^{\text{th}})^2)^{1/2}$  corresponds to the combined experimental and theoretical uncertainties. By means of the pull, we can compare the fitted values of each observable to their measured values. The  $\chi^2$  function is written as the sum of squared pulls, i.e.,

$$\chi^2 = \sum_i^{N_{\text{obs}}} (\text{pull}_i)^2, \quad (18)$$

where the sum extends over the number of observables ( $N_{\text{obs}}$ ) to be fitted. To account for the experimental correlation between  $R(D)$  and  $R(D^*)$ , we will use in our analysis the correlation value  $-0.38$  from HFLAV [26]. Likewise, we use the  $p$ -value to evaluate the fit-quality.

# Analysis on the TVB parametric space

Our analysis is based on the flavor observables presented in the previous Sec. ???. Let us recall that this dataset includes:  $b \rightarrow c\tau\bar{\nu}_\tau$  and  $b \rightarrow s\mu^+\mu^-$  data, bottomonium ratios  $R_{\Upsilon(nS)}$ , LFV decays ( $B^+ \rightarrow K^+\mu^\pm\tau^\mp$ ,  $B_s \rightarrow \mu^\pm\tau^\mp$ ,  $\Upsilon(nS) \rightarrow \mu^\pm\tau^\mp$ ), rare  $B$  decays ( $B \rightarrow K^{(*)}\nu\bar{\nu}$ ,  $B \rightarrow K\tau^+\tau^-$ ,  $B_s \rightarrow \tau^+\tau^-$ ), and  $\tau$  decays ( $\tau \rightarrow 3\mu$ ,  $\tau \rightarrow \mu\bar{\nu}_\mu\nu_\tau$ ). For the processes that only ULs have been experimentally reported so far, we will include them into the fit as a branching fraction of  $0 \pm \text{UL}/2$ . In addition, the  $B_s$  mixing and neutrino trident production are considered as constraints to be fulfilled. Our goal is to present an updated status of the TVB model as an explanation to the current  $b \rightarrow c\tau\bar{\nu}_\tau$  and  $b \rightarrow s\mu^+\mu^-$  data (referred by us as “*current data*”) hinting to LFU violation. In order to see the impact of the very recent LHCb measurement of  $R(\Lambda_c)$ , Eq. (??), into our analysis, we simply add  $R(\Lambda_c)$  to the *current data* observables (referred by us as “*current data* +  $R(\Lambda_c)$ ”).



# projections

Furthermore, taking into account the Belle II envisaged improvements on different observables previously discussed in Sec. ??, we investigate the impact of such sensitivities on the TVB model. For this purpose we will take the following considerations:

- Future Belle II sensitivities on the branching fraction of LFV decays ( $B^+ \rightarrow K^+ \mu^\pm \tau^\mp$ ,  $B_s \rightarrow \mu^\pm \tau^\mp$ ,  $\Upsilon(nS) \rightarrow \mu^\pm \tau^\mp$ ), and rare  $B$  decays ( $B \rightarrow K^{(*)} \nu \bar{\nu}$ ,  $B \rightarrow K \tau^+ \tau^-$ ,  $B_s \rightarrow \tau^+ \tau^-$ ).
- For the  $b \rightarrow s \mu^+ \mu^-$  data, we contemplate the future scenario with central values remaining the same, i.e., the  $b \rightarrow s \mu^+ \mu^-$  anomaly keeps in the future.
- With respect to  $b \bar{b} \rightarrow \tau^+ \tau^-$  processes, we assume that bottomonium leptonic decay ratios  $R_{\Upsilon(nS)}$  keep the central values, particularly, the recently obtained by BABAR on  $R_{\Upsilon(3S)}$ .
- Finally, as concerns the  $b \rightarrow c \tau \bar{\nu}_\tau$  data, we will pay particular attention to the Belle II prospects on  $R(D^{(*)})$  [27] by considering two plausible scenarios: (1) Belle II measurements on  $R(D^{(*)})$  keep the central values of Belle combination averages [28] with the projected Belle II sensitivities for  $50 \text{ ab}^{-1}$  and (2) Belle II measurements on  $R(D^{(*)})$  are reduced a 10% of the current central values of Belle combination averages (but still allowing small tension with the SM predictions) in conjunction with the projected Belle II sensitivities for  $50 \text{ ab}^{-1}$ . For the remaining  $b \rightarrow c \tau \bar{\nu}_\tau$  observables ( $R(J/\psi)$ , polarizations  $P_\tau(D^*)$  and  $F_L(D^*)$ ,  $R(X_c)$ , and  $R(\Lambda_c)$ ), we will assume that hold the same experimental values.

Regarding these two  $R(D^{(*)})$  scenarios along with other observables perspectives we will refer to these data set of projections as “Belle II-P1” and “Belle II-P2”, respectively. Such implications were not explored in the K LW analysis [3], neither in other recent works.

# Results

**Table:** Best-fit point values and  $1\sigma$  intervals of the five TVB couplings  $(g_{bs}^q, g_{bb}^q, g_{\mu\mu}^\ell, g_{\tau\tau}^\ell, g_{\mu\tau}^\ell)$  for  $M_V = 1$  TeV.

| TVB couplings                                   | Best-fit point        | $1\sigma$ intervals           |
|---|-----------------------|-------------------------------|
| <i>current data</i>                             |                       |                               |
| $g_{bs}^q$                                      | $-4.5 \times 10^{-3}$ | $[-5.8, -3.3] \times 10^{-3}$ |
| $g_{bb}^q$                                      | 2.54                  | [1.55, 3.52]                  |
| $g_{\mu\mu}^\ell$                               | 0.12                  | [0.09, 0.15]                  |
| $g_{\tau\tau}^\ell$                             | 0.45                  | [0.29, 0.60]                  |
| $g_{\mu\tau}^\ell$                              | $\sim 0$              | $[-0.14, 0.14]$               |
| <i>current data + <math>R(\Lambda_c)</math></i> |                       |                               |
| $g_{bs}^q$                                      | $-4.5 \times 10^{-3}$ | $[-5.6, -3.3] \times 10^{-3}$ |
| $g_{bb}^q$                                      | 2.43                  | [1.42, 3.42]                  |
| $g_{\mu\mu}^\ell$                               | 0.13                  | [0.09, 0.16]                  |
| $g_{\tau\tau}^\ell$                             | 0.43                  | [0.27, 0.59]                  |
| $g_{\mu\tau}^\ell$                              | $\sim 0$              | $[-0.14, 0.14]$               |

By fixing the TVB mass to the benchmark value  $M_V = 1$  TeV. For the *current data* we have a total of 26 observables, implying to a number of degrees of freedom of  $N_{\text{dof}} = 21$ . As for *current data +  $R(\Lambda_c)$* , we have 27 observables and  $N_{\text{dof}} = 22$ . For *current data* we get  $\chi_{\text{min}}^2 = 11.8$ , with a good fit of the data  $\chi_{\text{min}}^2/N_{\text{dof}} = 0.57$ . While for *current data +  $R(\Lambda_c)$* , we obtained  $\chi_{\text{min}}^2 = 14.6$  with a goodness  $\chi_{\text{min}}^2/N_{\text{dof}} = 0.67$

# Pulls

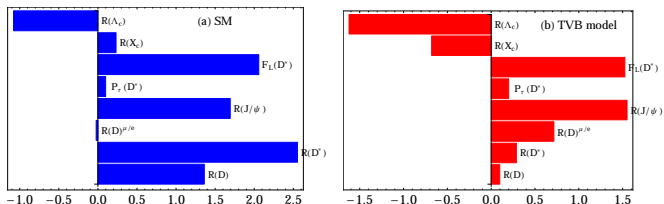
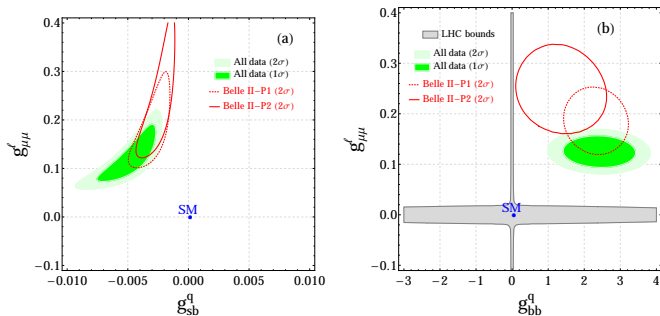


Figure: Pulls for (a) SM fit and (b) TVB model.



**Figure:** Allowed regions of the most relevant 2D parametric space of all data ( $current\ data + R(\Lambda_c)$ ) for  $M_V = 1\ TeV$ , where the  $1\sigma$  and  $2\sigma$  regions are shown in green and light-green colors, respectively. In each plot we are marginalizing over the rest of the parameters. The inner red dotted and red solid contours illustrate the permitted regions by projections Belle II-P1 and Belle II-P2, respectively. The SM value is represented by the blue circle. In panels (b) and (d), the light-gray region corresponds to LHC bounds at the 95% CL.

# LHC Constraints

By using the ATLAS search for high-mass dilepton resonances in the mass range of 250 GeV to 6 TeV, in proton-proton collisions at a center-of-mass energy of  $\sqrt{s} = 13$  TeV during Run 2 of the Large Hadron Collider (LHC) with an integrated luminosity of  $139 \text{ fb}^{-1}$  (ATLAS:2019erb), we obtain for  $M_V = 1$  TeV the lower limit on the parameter space from the intersection of the 95% CL upper limit on the cross-section from the the ATLAS experiment (ATLAS:2019erb). The TVB model has zero couplings to the first family to avoid the strong LHC constraints from the coupling between a  $Z'$  boson and valence quarks. The strongest restrictions come from  $Z'$  production processes in the  $b\bar{b}$  annihilation and the subsequent  $Z'$  decay into muons ( $\mu^+\mu^-$ ) and taus ( $\tau^+\tau^-$ ). TVB parameter space is limited by LHC constraints to regions where the couplings of the lepton or the quarks are close to zero, excluding the regions preferred by the  $B$  meson anomalies and low-energy flavor observables.

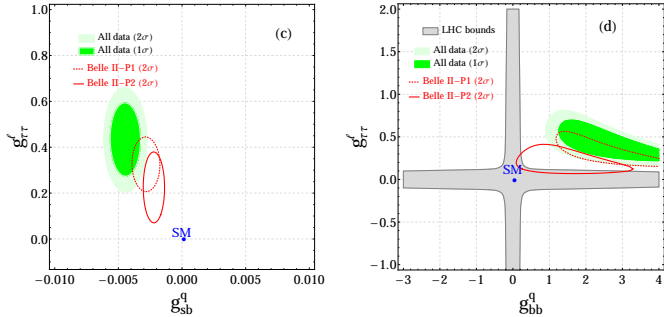







**Figure:** Allowed regions of the most relevant 2D parametric space of all data (*current data* +  $R(\Lambda_c)$ ) for  $M_V = 1$  TeV, where the  $1\sigma$  and  $2\sigma$  regions are shown in green and light-green colors, respectively. In each plot we are marginalizing over the rest of the parameters. The inner red dotted and red solid contours illustrate the permitted regions by projections Belle II-P1 and Belle II-P2, respectively. The SM value is represented by the blue circle. In panels (b) and (d), the light-gray region corresponds to LHC bounds at the 95% CL.

# Conclusions

- We have presented an updated view and perspectives of the triplet vector boson (TVB) model as a simultaneous explanation of the  $B$  meson anomalies ( $b \rightarrow c\tau\bar{\nu}_\tau$  and  $b \rightarrow s\mu^+\mu^-$  data). We performed a global fit of the parameter space of this model with the available 2022 data, including the very recent LHCb measurement on the ratio  $R(\Lambda_c) = \text{BR}(\Lambda_b \rightarrow \Lambda_c\tau\bar{\nu}_\tau)/\text{BR}(\Lambda_b \rightarrow \Lambda_c\mu\bar{\nu}_\mu)$  and global fit analyses of the most current  $b \rightarrow s\mu^+\mu^-$  data ( $C_9^{bs\mu\mu} = -C_{10}^{bs\mu\mu}$  solution).
- We have also included all relevant flavor observables such as  $B_s - \bar{B}_s$  mixing, neutrino trident production, LFV decays ( $B^+ \rightarrow K^+\mu^\pm\tau^\mp$ ,  $B_s \rightarrow \mu^\pm\tau^\mp$ ,  $\tau \rightarrow \mu\phi$ ,  $\Upsilon(nS) \rightarrow \mu^\pm\tau^\mp$ ), rare  $B$  decays ( $B \rightarrow K\nu\bar{\nu}$ ,  $B \rightarrow K\tau^+\tau^-$ ,  $B_s \rightarrow \tau^+\tau^-$ ), and bottomonium ratios  $R_{\Upsilon(nS)}$ ; as well as LHC bounds from searches of high-mass dilepton resonances at the ATLAS experiment. Additionally, we have studied the perspectives on TVB model by taking into account the expected Belle II future improvements on an extensive array of flavor processes, with special attention to the Belle II prospects on  $R(D^{(*)})$ .
- Our analysis has shown that although the TVB model can accommodate the  $b \rightarrow c\tau\bar{\nu}_\tau$  and  $b \rightarrow s\mu^+\mu^-$  anomalies (in consistency with other flavor observables), this seems to be strongly disfavoured by the LHC bounds. As concerns the future flavor data at Belle II, our findings suggest that the projected scenario in which the experimental measurement on  $R(D^{(*)})$  is reduced, it would allow a small NP window to solely explain the  $b \rightarrow c\tau\bar{\nu}_\tau$  data in agreement with LHC constraints.
- We have also studied the consequences of our analysis of the TVB model to flavor parametrizations in which the transformations involve only the second and third generations. We obtained that such a flavor ansatz is not viable within the TVB model.

# Frame Title

-  B. Bhattacharya, A. Datta, D. London, and S. Shivashankara, “Simultaneous Explanation of the  $R_K$  and  $R(D^{(*)})$  Puzzles,” *Phys. Lett. B*, vol. 742, pp. 370–374, 2015.
-  L. Calibbi, A. Crivellin, and T. Ota, “Effective Field Theory Approach to  $b \rightarrow s \ell \ell^{(\prime)}$ ,  $B \rightarrow K^{(*)} \nu \bar{\nu}$  and  $B \rightarrow D^{(*)} \tau \nu$  with Third Generation Couplings,” *Phys. Rev. Lett.*, vol. 115, p. 181801, 2015.
-  J. Kumar, D. London, and R. Watanabe, “Combined Explanations of the  $b \rightarrow s \mu^+ \mu^-$  and  $b \rightarrow c \tau^- \bar{\nu}$  Anomalies: a General Model Analysis,” *Phys. Rev. D*, vol. 99, no. 1, p. 015007, 2019.
-  D. A. Faroughy, A. Greljo, and J. F. Kamenik, “Confronting lepton flavor universality violation in B decays with high- $p_T$  tau lepton searches at LHC,” *Phys. Lett. B*, vol. 764, pp. 126–134, 2017.
-  A. Greljo, G. Isidori, and D. Marzocca, “On the breaking of Lepton Flavor Universality in B decays,” *JHEP*, vol. 07, p. 142, 2015.